Laser-Patterned n-Type Front-Junction Silicon Solar Cell With Tantalum Oxide/Silicon Nitride Passivation and Antireflection

Yimao Wan, Pei-Chieh Hsiao, Wei Zhang, Alison Lennon, Yifeng Chen, Zhiqiang Feng, Pierre Verlinden, Christian Samundsett, Jie Cui, Di Yan, and Andres Cuevas*

This work demonstrates, for the first time, a tantalum oxide/silicon nitride (Ta_2O_5/SiN_x) stack as a combined passivation and antireflection coating deposited on the boron-diffused front surface of n-type silicon solar cells. Due to the high chemical resistance of Ta_2O_5, the patterning of the films is realized via picosecond laser ablation, followed by a field-induced metal plating of nickel and copper to form the front metal grid electrode. A solar cell conversion efficiency of 19.3% is achieved, and further improvements are anticipated from the optimization of the laser ablation process and the tuning of the thickness of the individual layers of the dielectric stack.

The workhorse device for current industrial crystalline silicon (c-Si) photovoltaic (PV) manufacturing is still based on p-type silicon wafers. Nevertheless, as the silicon PV industry moves towards advanced high-efficiency solar cell concepts, n-type c-Si wafers are emerging as a preferred base material due to: 1) its higher tolerance to common metal impurities such as Fe,[1,2] and 2) the absence of light-induced degradation.[2,3] One of the n-type c-Si cell designs under most intensive evaluation for implementation in mass production is that based on front and rear dopant-diffused surfaces. A key requirement for this high efficiency n-type front-junction cell is highly effective passivation of the boron-diffused p^+ front surface. Passivation of such surfaces has historically been a major challenge in the PV industry, however it has become more feasible through the use of the negatively charged dielectric aluminum oxide (Al_2O_3).[4] Even more recently, several other dielectrics featuring negative charges have also been reported to provide a reasonable level of passivation to p^+ surfaces including titanium oxide,[5,6] aluminium nitride,[7,8] and gallium oxide.[9,10]

Recently, we have found that tantalum oxide (Ta_2O_5) stacked with silicon nitride (SiN_x) possesses a high density of negative charges ($\sim 10^{12}\,cm^{-2}$) and provides high quality passivation to p-type silicon surfaces.[11] By capping a ~12 nm thick Ta_2O_5 layer formed by atomic layer deposition (ALD) with a 85 nm SiN_x layer formed by plasma enhanced chemical vapor deposition (PECVD), we obtained a low recombination current density ($J_0 = 25\,fA\,cm^{-2}$) for boron-diffused ($\sim 150\,\Omega\,sq^{-1}$) p^+ c-Si wafers (including recombination within the diffused region). Furthermore, we demonstrated that the Ta_2O_5/SiN_x stack has excellent optical properties, with a relatively high refractive index and a negligible absorption of visible sunlight,[12] making it a promising dielectric for photovoltaic applications, both as a passivating and antireflection coating (ARC) layer. In this contribution, we further explore such applications by demonstrating a Ta_2O_5/SiN_x stack on a proof-of-concept n-type front-junction silicon solar cell.

Figure 1a outlines the schematic structure of the front-junction p^+nn^+ solar cell structure fabricated in this work. The solar cells were fabricated on float zone (FZ), n-type, 1 $\Omega\,cm^{-1}$ c-Si substrates, with a thickness of ~180 μm. After alkaline pyramidal texturing, a $\sim 120\,\Omega\,sq^{-1}$ p^+ region was formed on both sides of the wafer via boron diffusion from BBr_3. After etching the rear p^+ region, a $\sim 100\,\Omega\,sq^{-1}$ n^+ region was formed via full-area phosphorus diffusion from $POCl_3$. The p^+ front surface was then passivated by a 12 nm thermal ALD Ta_2O_5 film with the thickness tuned for minimising surface recombination, capped with a 62 nm SiN_x layer deposited at 300 °C by remote PECVD (AK400, Roth & Rou) for maximising photocurrent generation in the substrate.[12] On the n^+ diffused surface, an 85 nm thick SiN_x layer was deposited with the same PECVD equipment. A 1.2 μm layer of Ag was thermally evaporated onto the rear surface, which had been previously patterned by photolithography, to form localized rear point contacts covering 1% of the cell's rear surface area. Ta_2O_5 possesses high chemical

Dr. Y. Wan, C. Samundsett, Dr. J. Cui, Dr. D. Yan, Prof. A. Cuevas
Research School of Engineering
The Australian National University
Canberra, ACT 2601, Australia
E-mail: yimao.wan@anu.edu.au

Dr. P.-C. Hsiao, W. Zhang, A. Lennon
School of Photovoltaic and Renewable Energy Engineering
The University of New South Wales
Sydney 2052, Australia

Dr. Y. Chen, Dr. Z. Feng, Dr. P. Verlinden
State Key Lab of PV Science and Technology
Trina Solar Limited
No. 2 Trina Road, Trina PV Park, New District, Changzhou, Jiangsu 213031, China

DOI: 10.1002/solr.201700187

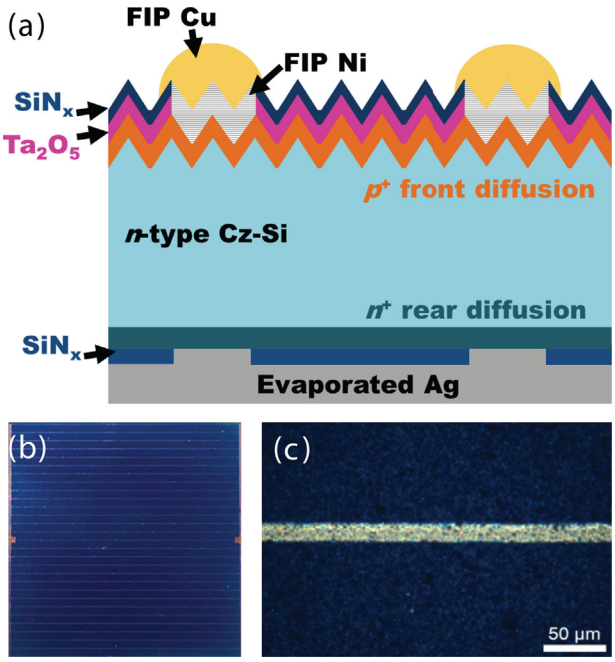

Figure 1. a) Schematic representation of front-junction p^+nn^+ silicon solar cell with front ALD Ta_2O_5/PECVD SiN_x ARC and rear PECVD SiN_x surface passivation; Optical microscope images of (b) a completed solar cell, and (c) a laser-ablated front finger opening.

stability in aqueous solutions over a range of pH values,[13–16] making it very challenging to pattern by chemical etching. The double dielectric front ARC coating was therefore patterned by laser scribing, using a 266 nm picosecond (ps) Lumera Super Rapid Nd:YAG laser with a BBO crystal for the 4th harmonic. Figure 1b and c show the optical microscope images of the complete solar cells and front laser ablated finger openings, respectively, showing the width of laser patterned finger to be ~10 µm. Following this, the front surface was deglazed to remove any residual surface oxide and metallized by field-induced plating (FIP)[17] of a nickel (Ni)/copper (Cu) stack using a single-side wet chemical plating apparatus. An approximately 1 µm thick layer of Ni and an 8 µm thick layer of Cu with a width of ~30 µm were plated onto the front surface to form a metal grid with a low metal series resistance.

The *J–V* photovoltaic characteristic curves were measured at standard testing conditions (AM1.5G spectrum, 100 mW cm^{-2}, 25 °C) using a solar simulator with constant, steady-state illumination, and the external quantum efficiency (EQE) was measured using a QE1400 (Protoflex) instrument. The reflectance was measured with a spectrophotometer (Lambda 1050, Perkin Elmer).

The effect of several process steps, namely passivation, patterning and plating, on the global recombination in the device was qualitatively evaluated by photoluminescence (PL) imaging of the solar cell under open circuit. The PL images shown in **Figure 2** indicate that the laser ablation step caused a significant deterioration of the passivation quality of the films, reducing the mean PL counts by more than half. Most likely this was a result of increased substrate temperature during the ablation process, leading to de-hydrogenation of the TaO_x film-silicon interface and/or local melting of the silicon surface.[18] As the solar cell was forward-biased during plating, it was expected that no deterioration of the front passivation would occur during the metallization process, and this is confirmed by the PL measurements.

The effect of laser ablation fluence was investigated by processing several complete silicon solar cells. **Table 1**

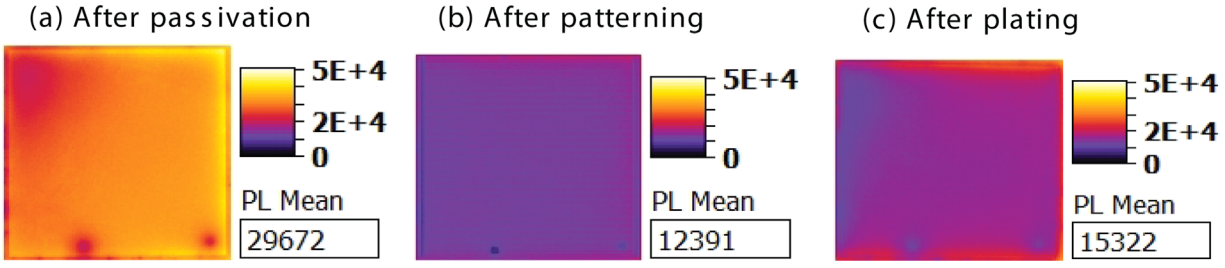

Figure 2. Open circuit PL images of the solar cells processed after (a) surface passivation, (b) laser patterning, and (c) field-induced plating.

Table 1. Summary of the cell results with different laser ablation pulse energy.

Pulse fluence ($J\,cm^{-2}$)	V_{OC} (mV)	J_{SC} ($mA\,cm^{-2}$)	FF (%)	pFF (%)	η (%)
1.5	634.2	37.71	80.84	81.2	19.33
2	630.5	37.53	80.55	81.1	19.06
2.2	628.5	36.85	79.71	80.2	18.46

summarizes the cell performance results, showing that, within the margin of error of the analysis, there was little effect on all cell parameters for the three laser pulse fluences investigated in this work (1.5, 2, and 2.2 $J\,cm^{-2}$, all single pass), although the lowest fluence gave the best results. The relatively low pseudo FF ($80.8 \pm 0.4\%$) measured by the Suns-V_{OC} method on finished cells may also be a consequence of laser induced defects.

The best cell in this work exhibits an open-circuit voltage (V_{OC}) of 634.2 mV, a short-circuit current (J_{SC}) of 37.71 $mA\,cm^{-2}$, a fill-factor (FF) of 80.84% and an efficiency of 19.3%, where the full current-voltage curve is displayed in **Figure 3**. The obtained device V_{OC} is significantly lower than the implied V_{OC} of the symmetrical Ta_2O_5/SiN_x passivated p^+ diffused sample (~680 mV).[11] This can be partly attributed to the increase in surface recombination induced by the laser ablation step. The J_{SC} is also relatively low, and this can be attributed to a non-optimal antireflection coating, as well as a de-passivation of the front surface, as will be discussed later in regard to the spectral response analysis. The high (close to the pseudo FF) measured fill factor implies that a contact with low series resistance has been realized via the laser ablation and the subsequent plated metallization. The inset in Figure 3 shows the measured spectral response of the best cell, including reflectance (R), external quantum efficiency (EQE), and internal quantum efficiency (IQE = EQE/[1–R]).

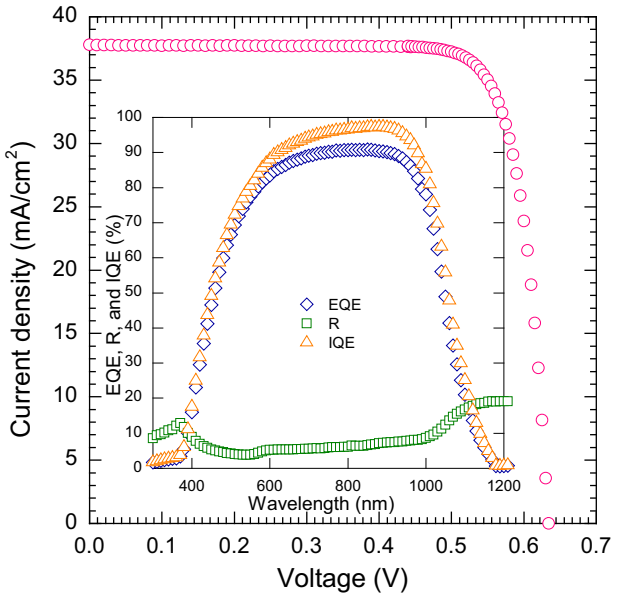

Figure 3. Measured light J–V behavior of the best cell measured under standard one sun conditions. The inset shows the external and internal quantum efficiencies accompanied by the measured reflectance for the cell.

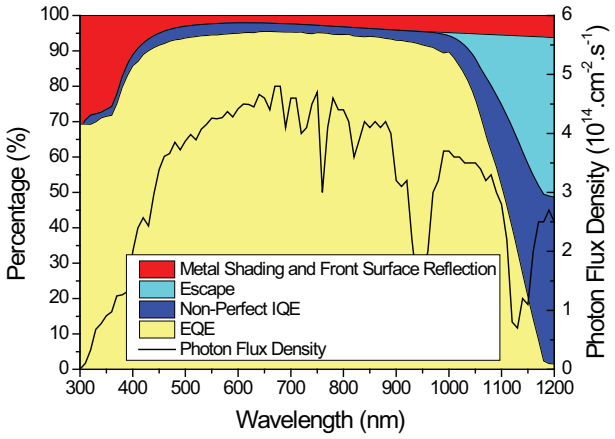

Figure 4. Optical loss analysis of the best cell shown in **Figure 3**. The dark blue region indicates recombination and parasitic absorption losses, and the red region indicates the optical loss due to front-surface reflection and metal shading. The loss analysis assumes an AM1.5G illumination spectrum, the photon flux of which is shown superimposed on the EQE data.

As we can see, the cell has a relatively poor collection efficiency (EQE < 80% at 500 nm) of short wavelength light (i.e., 400 to 600 nm). The two possible causes are 1) a non-optimum antireflection coating layer thickness, and 2) a high front surface recombination caused by the laser ablation step, as presented in Figure 2.

An analysis of the optical and parasitic absorption losses of the best cell in Table 1, based on that reported in Ref. [19], is graphically shown in **Figure 4** and summarized in **Table 2**. The red region in Figure 4 represents the loss due to metal shading and front surface reflection. The light blue region represents the losses due to the escape of long wavelength light from the front surface, showing the high reflectivity from the rear dielectric and silver metal. The dark blue region represents the light that is absorbed by the cell, but does not result in the generation of current (i.e., losses due to absorption of light by the Ta_2O_5/SiN_x ARC and recombination losses). These losses, referred to as non-perfect IQE losses in Figure 4, are the dominant loss of this cell.

Table 2. Summary of loss analysis of the best cell in **Table 1**.

Loss mechanism	Current density loss ($mA\,cm^{-2}$)	Power loss ($mW\,cm^{-2}$)
Optical loss (300–1200 nm)		1.90
Metal shading	1.98	1.07
Front surface reflection and escape	1.55	0.84
Resistance losses		0.61
R_S	n.a.	0.61
R_{SH}	n.a.	0.00
Recombination losses		3.87
Non-perfect IQE (300–1200 nm)	5.20	2.81
Forward-bias current at MPP	1.91	1.06
Total losses		6.38

The analysis clearly shows the possibility for further improvement of the front surface, both in terms of passivation and parasitic light absorption.

In conclusion, we have demonstrated, for the first time, a Ta_2O_5/SiN_x stack on front-junction n-type silicon solar cells as a passivation and antireflection coating, achieving a conversion efficiency of 19.3%. The front finger contacts were made via ps laser ablation and field-induced plating of Ni and Cu. Further improvements can be expected through optimising the laser ablation process and tuning the thickness of the individual layers in the dielectric stack.

Acknowledgments

This work has been supported by the Australian government through the Australian Renewable Energy Agency (ARENA) and by Trina Solar (No: 2014/RND003).

Conflict of Interest

The authors declare no conflict of interest.

Keywords

antireflection, passivation, silicon nitride, silicon solar cells, tantalum oxide

Received: November 1, 2017
Revised: November 22, 2017
Published online: January 16, 2018

[1] D. Macdonald, L. J. Geerligs, *Appl. Phys. Lett.* **2004**, *85*, 4061.
[2] J. Schmidt, K. Bothe, *Phys. Rev. B* **2004**, *69*, 024107.
[3] J. Zhao, A. Wang, M. A. Green, *Prog. Photovoltaics: Res. Appl.* **2000**, *8*, 549.
[4] B. Hoex, J. Schmidt, R. Bock, P. P. Altermatt, M. C. M. van de Sanden, W. M. M. Kessels, *Appl. Phys. Lett.* **2007**, *91*, 112107.
[5] J. Cui, T. Allen, Y. Wan, J. Mckeon, C. Samundsett, D. Yan, X. Zhang, Y. Cui, Y. Chen, P. Verlinden, *Sol. Energy Mater. Sol. Cells* **2016**, *158*, 115.
[6] A. F. Thomson, K. R. McIntosh, *Prog. Photovoltaics: Res. Appl.* **2012**, *20*, 343.
[7] G. Krugel, A. Sharma, W. Wolke, J. Rentsch, R. Preu, *Phys Status Solidi (RRL) – Rapid Res. Lett.* **2013**, *7*, 457.
[8] G. Krugel, A. Sharma, A. Moldovan, W. Wolke, J. Rentsch, and R. Preu, presented at the Photovoltaic Specialists Conference (PVSC), 2013 IEEE 39th, **2013**.
[9] T. G. Allen, Y. Wan, A. Cuevas, *IEEE J. Photovoltaics* **2016**, *6*, 900.
[10] T. G. Allen, A. Cuevas, *Appl. Phys. Lett.* **2014**, *105*, 031601.
[11] Y. Wan, J. Bullock, A. Cuevas, *Appl. Phys. Lett.* **2015**, *106*, 201601.
[12] Y. Wan, J. Bullock, A. Cuevas, *Sol. Energy Mater. Sol. Cells* **2015**, *142*, 42.
[13] M. D. Anderson, B. Aitchison, D. C. Johnson, *ACS Appl. Mater. Interfaces* **2016**, *8*, 30644.
[14] C. Li, T. Wang, Z. Luo, D. Zhang, J. Gong, *Chem. Commun.* **2015**, *51*, 7290.
[15] S. Chen, L.-W. Wang, *Chem. Mater.* **2012**, *24*, 3659.
[16] S. Hu, N. S. Lewis, J. W. Ager, J. Yang, J. R. McKone, N. C. Strandwitz, *J. Phys. Chem. C* **2015**, *119*, 24201.
[17] X. Wang, V. Allen, V. Vais, Y. Zhao, B. Tjahjono, Y. Yao, S. Wenham, A. Lennon, *Sol. Energy Mater. Sol. Cells* **2014**, *131*, 37.
[18] D. Walter, A. Fell, E. Franklin, D. Wang, K. Fong, T. Kho, K. Weber, A. W. Blakers, *Sol. Energy Mater. Sol. Cells* **2015**, *136*, 1.
[19] A. G. Aberle, W. Zhang, B. Hoex, *Energy Procedia* **2011**, *8*, 244.